## FULL PAPER

# Metal artefact reduction in CT imaging of hip prostheses— an evaluation of commercial techniques provided by four vendors

[1]K M ANDERSSON, Msc, [2]P NOWIK, Msc, [1]J PERSLIDEN, PhD, [1,3]P THUNBERG, PhD and [1]E NORRMAN, PhD

[1]Department of Medical Physics, Faculty of Medicine and Health, Örebro University, Örebro, Sweden
[2]Department of Medical Physics, Karolinska University Hospital, Stockholm, Sweden
[3]School of Health and Medical Sciences, Örebro University, Örebro, Sweden

Address correspondence to: Ms Karin M Andersson
E-mail: karin.andersson@regionorebrolan.se

**Objective:** The aim of this study was to evaluate commercial metal artefact reduction (MAR) techniques in X-ray CT imaging of hip prostheses.

**Methods:** Monoenergetic reconstructions of dual-energy CT (DECT) data and several different MAR algorithms, combined with single-energy CT or DECT, were evaluated by imaging a bilateral hip prosthesis phantom. The MAR images were compared with uncorrected images based on CT number accuracy and noise in different regions of interest.

**Results:** The three MAR algorithms studied implied a general noise reduction (up to 67%, 74% and 77%) and an improvement in CT number accuracy, both in regions close to the prostheses and between the two prostheses. The application of monoenergetic reconstruction, without any

MAR algorithm, did not decrease the noise in the regions close to the prostheses to the same extent as did the MAR algorithms and even increased the noise in the region between the prostheses.

**Conclusion:** The MAR algorithms evaluated generally improved CT number accuracy and substantially reduced the noise in the hip prostheses phantom images, both close to the prostheses and between the two prostheses. The study showed that the monoenergetic reconstructions evaluated did not sufficiently reduce the severe metal artefact caused by large orthopaedic implants.

**Advances in knowledge:** This study evaluates several commercially available MAR techniques in CT imaging of large orthopaedic implants.

Images degraded by metal artefacts are a common problem in X-ray CT imaging. Artefacts caused by the presence of metallic implants in the CT scanned volume, such as hip prostheses or dental fillings, appear as dark and bright streaks across the reconstructed image. Metal artefacts can severely degrade the image quality and hence limit the diagnostic value of a CT scan.[1]

Hip prostheses cause severe artefacts when present in a CT scanned volume, and the resulting degradation of image quality leads to difficulties in diagnosing fractures, implant loosening or pathology in organs or soft tissue in the pelvic area. If CT images containing hip prostheses are used in radiotherapy treatment planning for tissue heterogeneity correction, the metal artefacts may introduce inaccuracies in dose calculations.

Metal artefacts in CT imaging are mainly caused by beam hardening and photon starvation. Photon starvation artefacts are created when X-rays traverse materials with high

attenuation coefficients, which leads to an insufficient amount of photons reaching the detectors and results in very noisy projections. The noise is magnified in the reconstruction process and the resulting streaks can be seen in the reconstructed image. Beam hardening refers to the fact that low-energy photons are attenuated to a greater degree than high-energy photons when passing through the scanned volume. This effect is more pronounced when the X-ray beam passes through high-density materials such as metals.[1]

In the past, several case-by-case solutions have been used in clinics to reduce metal artefacts. These are most often insufficient. One approach is to increase the tube peak voltage; however, this may only reduce metal artefact degradation to a minor degree and may not improve imaging of larger implants such as hip prostheses.[2] Increasing tube current, on the other hand, would lead to a higher radiation dose to the patient and may not have considerable impact on image quality either.[2] Approaches such as gantry tilting, or using

lower attenuating materials in implants to avoid metal artefacts, may only be possible in specific situations and are effective to a limited extent.[3,4] Several proposed metal artefact reduction (MAR) algorithms working on raw projection data, such as modified iterative reconstruction (IR) methods and projection interpolation algorithms, have been shown to be a more general and effective technique for reducing artefacts.[4]

Dual-energy CT (DECT) imaging enables image reconstruction from two energy sources and thereby creation of simulated monoenergetic images. This application makes it possible to obtain images as though they had been acquired with a monoenergetic high-energy beam, which would lead to reduction of metal artefacts caused by beam hardening.[5–9]

In addition to monoenergetic reconstructions in DECT, dedicated MAR algorithms have become available for clinical practice in the past couple of years. MAR algorithms in both single-energy CT imaging[10–14] and DECT imaging[8,9] have been shown to reduce metal artefacts.

Some of the commercially available MAR techniques have previously been studied for several different clinical examples, ranging from artefacts created by smaller metallic objects such as dental fillings or screws to larger implants such as hip prostheses.[5–13] Monoenergetic images, reconstructed from DECT data, have been shown to enhance the diagnostic value of CT images containing orthopaedic implants.[5–10] Li et al[12] studied the application of a commercially available MAR algorithm in radiotherapy treatment planning and concluded that it improved CT number accuracy and structure visualization in CT images of orthopaedic implants. However, the improvement in CT number accuracy was shown not to have any significant clinical impact on photon dose calculations. A study by Andersson et al[13] showed that the same MAR algorithm improves the accuracy in proton dose calculations.

The aim of this study was to evaluate how the MAR techniques for CT scanners from four different vendors impact the diagnostic value of CT studies of hip prostheses, using a consistent experimental set-up for all machines. All CT images were evaluated in the same way, that is, by measuring CT number accuracy and noise in different regions of the images. Several scan parameters were varied to study their effect on MAR.

## METHODS AND MATERIALS
### Phantom imaging
With the help of an orthopaedic surgeon, two chromium–cobalt prostheses were mounted in the hip and femur bones of a calf, which were then jointly placed in a water-filled phantom (Figure 1). The phantom had a cross section of $40 \times 50 \text{ cm}^2$ and was filled up to 20 cm with water. A plastic slab and plastic rods were used to centre the hip prostheses in the phantom. Rods were also placed adjacent to the bones as a guide for placing the prostheses in the same position for every CT scan, to the extent possible.

Four CT scanners from four different vendors were used in the study: Philips Ingenuity Core (Philips Healthcare, Cleveland, OH); Toshiba Aquilion ONE™ Vision Edition (Toshiba Medical Systems, Otawara, Japan); GE Discovery™ 750HD (GE Healthcare,

Figure 1. The phantom with hip prostheses mounted in bones of a calf. The phantom had a cross section of $40 \times 50 \text{ cm}^2$ and was filled up to 20 cm with water during the CT scans.



Milwaukee, WI); and Siemens SOMATOM® Definition Flash (Siemens Healthcare, Forchheim, Germany). For every CT scanner, the hip prostheses phantom was scanned with a tube peak voltage of 120 kVp, without using any MAR technique (hereafter called uncorrected images). The hip prostheses phantom was also scanned with the specific MAR technique for each CT scanner. The uncorrected CT images were then compared with the metal artefact-reduced images, in terms of CT number accuracy and noise.

A constant $CTDI_{vol32}$ value (volume CT dose index) of 28 mGy was used during all scans with the four different CT scanners, by manually adjusting the tube current. A reconstructed slice thickness of 2 mm with an increment of 1 mm, a reconstruction field of view of 420 mm and a $512 \times 512$ pixels image matrix were used for all images. Helical CT protocols, where the pitch was set to approximately 0.5, were used for all CT scanners, except for the Toshiba CT scanner where the MAR algorithm (SEMAR) is only compatible with volume scanning protocols.

The reconstruction technique [filtered backprojection (FB) or IR] and reconstruction kernel (soft or sharper) were varied in the phantom images. The different settings were used combined with the MAR techniques and the uncorrected images. In the case of IR, an intermediate level of the IR algorithm, installed on the CT scanner in question, was used in the images. The choice of the soft and the sharper reconstruction kernels was made for each CT scanner based on the kernels that are commonly used in the hospital's clinic for CT examinations in the pelvic area. The CT scan parameters for the four CT scanners are summarized in Table 1.

When reconstructing monoenergetic images from DECT data, the operator has the potential to choose the extrapolated energy level to be used. A DECT protocol optimization study by Meinel et al[6] showed that optimal MAR was seen when using a monoenergetic

Table 1. CT scan parameters used in the study, for the four different CT scanners

| Parameter | Philips Ingenuity Core (single energy) [Philips (Cleveland, OH)] | Toshiba Aquilion ONE™ Vision Edition (single energy) [Toshiba (Otawara, Japan)] | GE Discovery™ 750HD (dual energy by fast kilovoltage switching) [GE (Milwaukee, WI)] | Siemens SOMATOM® Definition Flash (dual energy with dual sources) [Siemens (Forchheim, Germany)] |
|---|---|---|---|---|
| CT protocol | Helical | Volume | Helical | Helical |
| Collimation (mm) | 64 × 0.625 | 280 × 0.5 | 64 × 0.625 | 64 × 0.6 |
| MAR technique | MAR algorithm (O-MAR) | MAR algorithm (SEMAR) | Monoenergetic reconstruction (110 keV) MAR algorithm (MARS) | Monoenergetic reconstruction (110 keV) DE-composition reconstructions (weight of −0.3) |
| Iterative reconstruction | iDose | AIDR 3D (adaptive iterative dose reduction 3D) | ASIR (adaptive statistical iterative reconstruction) | SAFIRE (sinogram affirmed iterative reconstruction) |
| | Level 3 (range, 1–5) | Level standard (range, mid, standard and strong) | Level 50% (range, 0–100%) | Level 3 (range, 1–5) |
| Soft kernel | B | FC08 | Standard | D34 (FB) Q30 (IR) |
| Sharper kernel | YB | FC30 | Detail | D45 (FB) Q50 (IR) |

FB, filtered backprojection; IR, iterative reconstruction; MAR, metal artefact reduction; MARS, metal artefact reduction software; O-MAR, MAR for orthopaedic implants; SEMAR, single-energy MAR.

level of between 105 and 120 keV. Recommendations from application specialists from the different CT scanner vendors and from radiologists in the hospital's clinic reasonably coincided with this conclusion. Based on these facts, a monoenergetic level of 110 keV was used in this study.

## Scanner-specific metal artefact reduction techniques
### Philips Ingenuity Core CT
The Philips Ingenuity Core single-energy CT used in this study uses a MAR algorithm called metal artefact reduction for orthopaedic implants (O-MAR). O-MAR is an iterative projection modification method optimized for imaging orthopaedic devices. The CT image acquired with the scanner is used as input into an iterative loop, where the output is a correction image that is subtracted from the input image. O-MAR uses segmentation and replaces data points identified as metal with interpolated values. When using the O-MAR algorithm, an uncorrected data volume is always automatically reconstructed.[15]

### Toshiba Aquilion ONE CT
The Toshiba Aquilion ONE Vision Edition single-energy CT scanner uses a MAR algorithm called single-energy metal artefact reduction (SEMAR). SEMAR is only applicable for volume scans in the software version installed on the CT scanner evaluated in this study (v. 6.0). The volume scan covers a maximum range of 160 mm in one single axial scan. According to the vendor, SEMAR uses segmentation of the images and correction of raw data to reduce metal artefacts. Images were acquired and analysed both with and without SEMAR.

### GE Discovery 750HD CT
The GE Discovery 750HD CT is a single-source DECT with fast kilovoltage switching between 80 and 140 kVp in 0.25 ms. The GE CT can combine the monoenergetic image reconstruction with a metal artefact reduction software (MARS). According to the vendor, the MARS algorithm is designed to correct for extreme beam-hardening artefacts under severe low-signal conditions owing to photon starvation. MARS uses segmentation of the high intensity measurements and replaces missing data owing to low signal with data derived from accurate projection measurements.

### Siemens SOMATOM Definition Flash CT
The Siemens SOMATOM Definition Flash CT is a dual-source DECT with the capability to create monoenergetic images. When acquiring the DECT images, a spectral combination of 140 kVp hardened with a 0.1-mm tin filter and 100 kVp (100/Sn140 kVp) was used. In addition to the monoenergetic reconstructions, which were obtained from image analysis at a separate workstation, the Siemens CT uses an application for reducing metal artefacts directly at the CT scanner. This application is called DE-composition and adjusts the weighting of the 140-kVp spectrum data and the 100-kVp spectrum data in the reconstructed image. The images obtained with the DE composition application are reconstructed based on the same principle as the monoenergetic reconstructions, but this application uses an additional noise reduction filter. The DE composition value is manually chosen by the user on a scale from −1.0 to 1.0. A DE composition value of −0.3 is used in the hospital's clinic for imaging orthopaedic implants and was therefore also used in this study.

## Image analysis

The CT numbers in the images were analysed in MATLAB® (Mathworks®, Natick, MA) by evaluating the regions of interest (ROIs) in the images. An axial CT slice positioned in the middle of the hip prostheses' heads was used for analysis in all CT series. The mean value of the CT numbers and the noise (CT number standard deviation) in three ROIs were calculated for both the uncorrected images and the MAR images. Two ROIs were located adjacent to the hip prostheses' heads (ROI1, ROI2) and a third ROI was located across the low-density zone between the hip prostheses (ROI3) (Figure 2). The positions of the ROIs were chosen based on clinical relevance. Artefacts close to the prostheses may hamper the diagnosis of prosthesis loosening, for example. Artefacts in the area between the two prostheses may degrade the depiction of the bladder or the prostate, for example.

The arrangement of the bones containing the hip implants was approximately the same for every CT scanner. The ROIs were placed in approximately the same position relative to the bones and the prostheses in the images from all scanners. The ROI1 and ROI2 consisted of circle sectors that were placed at the same location relative to the hip prostheses heads for all CT scanners. The ROI3 consisted of a circle with the same size and relative position for all machines. The ROIs were consistently placed in phantom areas only containing water.

## RESULTS

Figure 2 shows CT images of the hip prostheses phantom, acquired with the four different CT scanners. All images shown are reconstructed with FB and a soft reconstruction kernel. A window width of 1400 HU and a window level of 300 HU are used for displaying the images through the paper. Figure 3 shows the result of CT number accuracy and noise level evaluation in the ROIs in the phantom images acquired with the four CT scanners.

The results show that when the MAR algorithms (O-MAR, SEMAR and MARS) were used, the noise was generally reduced in the ROIs. The only exception to this is when the sharper reconstruction kernel was combined with FB for the Toshiba CT images. In this case, the use of the SEMAR algorithm resulted in increased noise in ROI2 and ROI3 compared with the uncorrected image. In the monoenergetic images from the Siemens CT and the GE CT (without the MARS algorithm), the noise was reduced in ROI1 and ROI2, but increased in ROI3, compared with the corresponding uncorrected images.

In the Philips CT images, the noise was reduced by up to 53% in ROI1, by up to 66% in ROI2 and by up to 65% in ROI3 when O-MAR was used, compared with the uncorrected images. In

Figure 2. CT images of the hip prostheses shown for the CT scanners from four different vendors: Philips Healthcare (Cleveland, OH), Toshiba Medical Systems (Otawara, Japan), GE Healthcare (Milwaukee, WI), and Siemens Healthcare (Forchheim, Germany) (for details, see Table 1). The first column shows the uncorrected images acquired with a tube voltage of 120 kVp with the three regions of interest marked. The second and third columns show the images obtained with the different metal artefact reduction (MAR) techniques (MAR algorithms and/or monoenergetic reconstructions of dual-energy (DE) CT data). All images shown are reconstructed with filtered backprojection and a soft reconstruction kernel. A window width of 1400 and a window level of 300 are used for displaying the images. MARS, metal artefact reduction software; O-MAR, MAR for orthopaedic implants; SE, single energy; SEMAR, single-energy MAR.
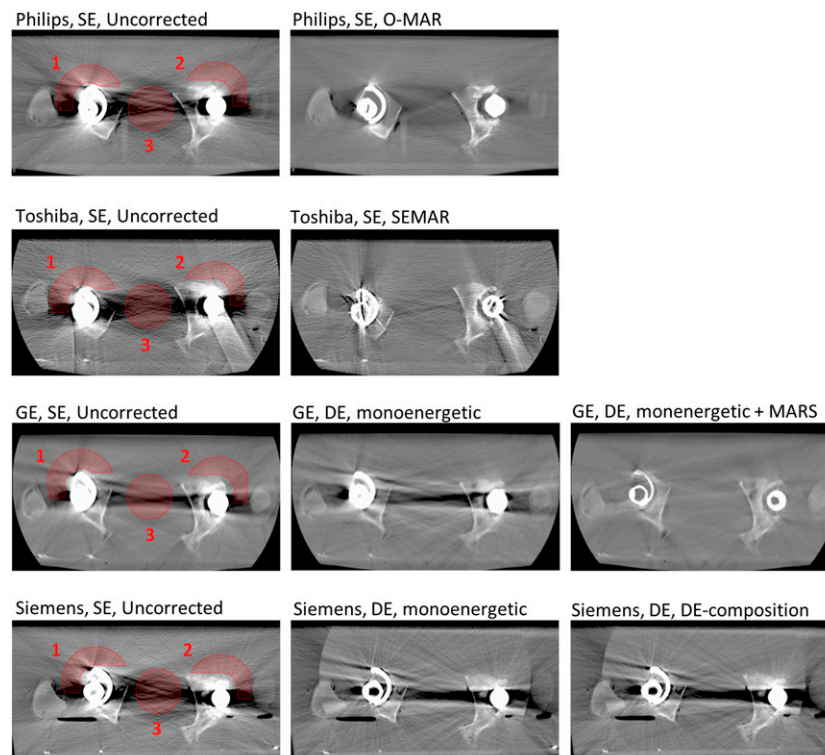
Figure 3. (a–d) Mean value and the noise (standard deviation) of the CT numbers in the regions of interest (ROIs) (marked in Figure 2), for the phantom scanned with CTs from the four vendors: Philips Healthcare (Cleveland, OH) (a), Toshiba Medical Systems (Otawara, Japan) (b), GE Healthcare (Milwaukee, WI) (c), and Siemens Healthcare (Forchheim, Germany) (d). The standard deviation values are marked by grey areas (white for ROI1, lighter grey for ROI2 and darker grey for ROI3). In each box the mean values are marked by solid lines. The values are shown for the different reconstruction settings; soft/sharper kernel and filtered backprojection/iterative reconstruction. For CT scanner and scan parameter details, see Table 1. DE-comp, DE-composition; MARS, metal artefact reduction software; mono, monoenergetic reconstruction; O-MAR, metal artefact reduction for orthopaedic implants; SEMAR, single-energy metal artefact reduction; Uncorr, uncorrected.
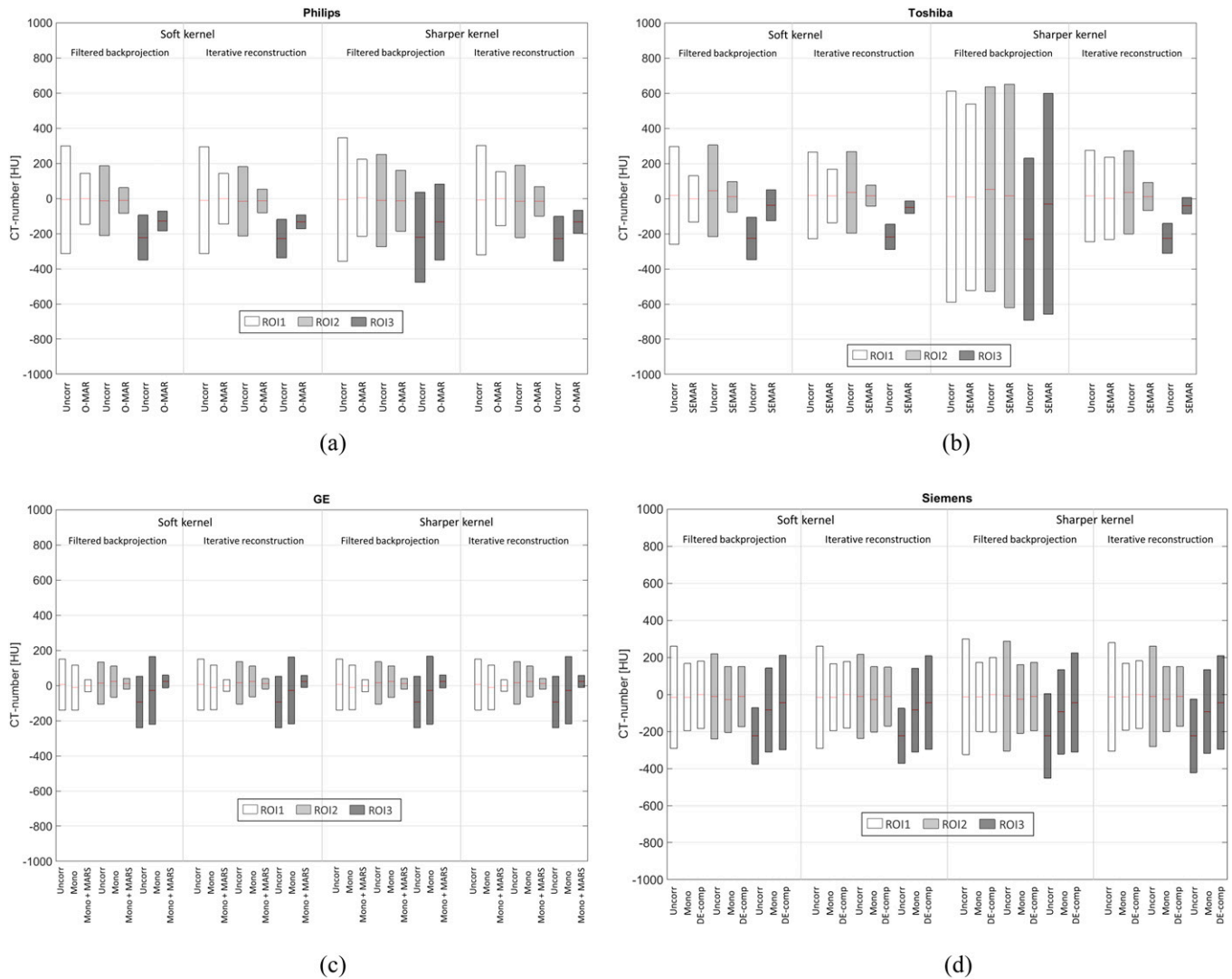


the Toshiba images, the noise was reduced by up to 52% in ROI1, by up to 75% in ROI2 and by up to 50% in ROI3 when SEMAR was used, compared with the uncorrected images. In the GE CT images in which monoenergetic reconstructions were combined with MARS, the decrease in noise was between 75% and 77% in all of the ROIs.

When monoenergetic reconstruction without the MARS algorithm was used for the GE CT data, the noise was decreased by up to 12% in ROI1 and by up to 27% in ROI2. In ROI3, the noise was increased by up to 32%, compared with the uncorrected images. The monoenergetic images acquired with the Siemens CT showed a decrease in noise up to 41% in ROI1 and by up to 37% in ROI2. The corresponding values for the DE-composition images were

39% and 41%. In ROI3, on the other hand, the noise levels were increased by up to 52% in the monoenergetic images and by up to 70% in the DE-composition images.

The results show that in ROI3, where the mean values of the CT numbers were between −100 and −230 HU in the uncorrected images for all scanners, the mean values were generally closer to zero in the MAR algorithm images than in uncorrected images. This is also true for the monoenergetic reconstructions; however, in these images, the noise in ROI3 was increased compared with the uncorrected images, which suggests a general degradation of image quality rather than an improvement. In ROI1 and ROI2, the mean values in the uncorrected images were already close to zero, and when the

MAR techniques were used, the mean values were improved or stayed approximately unchanged.

The different reconstruction techniques (FB or IR) and reconstruction kernels (soft or sharper) affected the images in different ways for the four CT scanners. In the case of the GE CT images, the noise only changed to a small extent with different reconstruction techniques and kernels. For the Philips CT images, the O-MAR image acquired with FB and a sharper kernel showed the least reduction in noise when compared with a corresponding reference image (38% in ROI1, 34% in ROI2 and 16% in ROI3) of all settings. The O-MAR image reconstructed with a soft kernel and IR showed the greatest reduction (53% in ROI1, 66% in ROI2 and 65% in ROI3).

In the case of the Toshiba CT images, the noise in ROI2 and ROI3 was increased in the SEMAR image reconstructed with a sharper kernel and FB, compared with the corresponding uncorrected image (9% and 36%, respectively). The Toshiba images reconstructed with a soft kernel and IR show the greatest reduction in noise for ROI2 and ROI3 (75% and 50%, respectively) of all settings. In ROI1, however, the reduction in noise when using SEMAR was larger for the soft-kernel FB image than for the soft-kernel IR image (52% compared with 38%). In the Toshiba image reconstructed with a sharper kernel and IR, the noise level in ROI1 was approximately the same for the SEMAR image and the uncorrected image, which deviates from the corresponding results for ROI2 and ROI3. ROI1 is placed adjacent to the right prosthesis, where both a metallic head and a metallic cup are present (compared with the plastic cup of the left prosthesis). When the SEMAR algorithm was used, new high-density streaks originating from metal were seen, especially on the right side. These additional streaks were particularly obvious when the SEMAR algorithm was combined with IR, which correlates with the measured noise levels.

## DISCUSSION
The O-MAR algorithm used with Philips CT has previously been shown to improve CT number accuracy in images of orthopaedic implants.[10,12] The monoenergetic reconstructions obtained from Siemens DECT[5–7] and GE DECT[8,9] (in combination with MARS in the case of GE) have also been shown to reduce metal artefacts effectively.

The result of this study shows that CT number accuracy was generally improved and the noise was generally reduced in the ROIs of the hip prostheses phantom images, when the O-MAR algorithm was used for the Philips CT images, when the SEMAR algorithm was used for the Toshiba CT images and when the MARS algorithm was used for the GE CT images.

In this study, the use of monoenergetic reconstructions, without any MAR algorithm, increased the noise in the ROI between the prostheses. The noise in the ROIs close to the prostheses was reduced when the monoenergetic reconstructions were used, but not to the same extent as in the images reconstructed with the MAR algorithms.

Monoenergetic reconstructions have previously been concluded to effectively reduce artefacts from larger metallic implants.[5–7]

The finding of this study—that monoenergetic reconstructions could increase the noise in some regions of the image—deviates from those of the previous studies. An explanation for this may be various clinical situations considered, which in turn means a different experimental set-up, such as the phantom design (unilateral/bilateral prostheses and/or varying prostheses material) or evaluation of different image areas.

Monoenergetic reconstruction is utilized to reduce artefacts caused by beam hardening. However, metal artefacts are also caused by photon starvation. This study shows that using monoenergetic reconstruction alone is not sufficient for reducing severe artefacts caused by large orthopaedic implants. This fact was clearly seen in this study when using the monoenergetic reconstructions of the GE DECT data—both alone and in combination with the MARS algorithm. When monoenergetic reconstruction was used alone, the noise increased between the prostheses (32%) and decreased, to a modest extent, close to the prostheses (12–27%). When monoenergetic reconstruction was combined with the MARS algorithm, designed to reduce artefacts caused by beam hardening under severe photon starvation conditions, the noise was reduced by approximately 75% in all regions evaluated.

To be able to obtain a complete evaluation of these MAR techniques, it would be of interest to perform a qualitative image analysis as a complement to the quantitative CT number analysis carried out in this study. A visual grading study of these kinds of images, based on the diagnostic question considered, would be complementary to this study.

The creation of new artefacts when using commercial MAR software has previously been reported[16] and was also seen in this study. New high-density streaks, originating from the metallic cup and head, were created when using the SEMAR algorithm in this study. These additional artefacts were particularly obvious when the SEMAR algorithm was combined with IR. These additional artefacts could be further analysed in a visual grading study.

Since the same CTDI value was used for all CT scanners evaluated, which included both single-energy CT/DECT and helical/volume scanning protocols, no dose optimization of the scan protocols for each specific CT scanner has been made in respect of MAR. Another limitation of this study may be the fact that only one level of IR was used. Optimization of the CT protocol in terms of the IR level is of course important, and further investigations should be made into the effect of IRs on metal artefact-degraded images. MAR in CT imaging of hip prostheses material other than chromium–cobalt may also be of interest for further study.

## CONCLUSION
From this bilateral hip prosthesis phantom study, it was concluded that using the O-MAR algorithm (Philips Ingenuity Core CT), the SEMAR algorithm (Toshiba Aquilion ONE Vision Edition CT) and the MARS algorithm combined with monoenergetic reconstruction of DECT data (GE Discovery 750HD CT) improved CT number accuracy and led to a decrease in noise in ROIs both adjacent to the head of the prostheses and also between the prostheses, compared with corresponding uncorrected CT images.

The use of monoenergetic reconstruction alone (tested with Siemens SOMATOM Definition Flash CT and GE Discovery 750HD CT), without any additional MAR algorithm, did not decrease the noise in the regions adjacent to the head of the prostheses to the same extent as the MAR algorithms, and actually increased the noise in the region between the two prostheses.

## REFERENCES

1. Barrett JF, Keat N. Artefacts in CT: recognition and avoidance. *Radiographics* 2004; **24**: 1679–91. doi: 10.1148/rg.246045065

2. Lee MJ, Kim S, Lee SA, Song HT, Huh YM, Kim DH, et al. Overcoming artifacts from metallic orthopedic implants at high-field-strength MR imaging and multi-detector CT. *Radiographics* 2007; **27**: 791–803.

3. Naka Y, Sakamoto K, Minamoto T, Kamakura T, Ogata Y, Matsumoto M, et al. Clinical evaluation of a newly developed method for avoiding artifacts caused by dental fillings on X-ray CT. *Radiol Phys Technol* 2008; **1**: 115–22. doi: 10.1007/s12194-007-0016-8

4. Yazdi M, Gingras L, Beaulieu L. An adaptive approach to metal artifact reduction in helical computed tomography for radiation therapy treatment planning: experimental and clinical studies. *Int J Radiat Oncol Biol Phys* 2005; **62**: 1224–31.

5. Lewis M, Reid K, Toms AP. Reducing the effects of metal artefact using high keV monoenergetic reconstruction of dual energy CT (DECT) in hip replacements. *Skeletal Radiol* 2013; **42**: 275–82. doi: 10.1007/s00256-012-1458-6

6. Meinel FG, Bischoff B, Zhang Q, Bamberg F, Reiser MF, Johnson TR. Metal artifact reduction by dual-energy computed tomography using energetic extrapolation: a systematically optimized protocol. *Invest Radiol* 2012; **47**: 406–14. doi: 10.1097/RLI.0b013e31824c86a3

7. Bamberg F, Dierks A, Nikolaou K, Reiser MF, Becker CR, Johnson TR. Metal artifact reduction by dual energy computed tomography using monoenergetic extrapolation. *Eur Radiol* 2011; **21**: 1424–9. doi: 10.1007/s00330-011-2062-1

8. Pessis E, Campagna R, Sverzut JM, Bach F, Rodallec M, Guerini H, et al. Virtual monochromatic spectral imaging with fast kilovoltage switching: reduction of metal artifacts at CT. *Radiographics* 2013; **33**: 573–83. doi: 10.1148/rg.332125124

9. Lee YH, Park KK, Song HT, Kim S, Suh JS. Metal artefact reduction in gemstone spectral imaging dual-energy CT with and without metal artefact reduction software. *Eur Radiol* 2012; **22**: 1331–40. doi: 10.1007/s00330-011-2370-5

10. Hilgers G, Nuver T, Minken A. The CT number accuracy of a novel commercial metal artifact reduction algorithm for large orthopedic implants. *J Appl Clin Med Phys* 2014; **15**: 4597. doi: 10.1120/jacmp.v15i1.4597

11. Kidoh M, Nakaura T, Nakamura S, Tokuyasu S, Osakabe H, Harada K, et al. Reduction of dental metallic artefacts in CT: value of a newly developed algorithm for metal artefact reduction (O-MAR). *Clin Radiol* 2014; **69**: e11–16. doi: 10.1016/j.crad.2013.08.008

12. Li H, Noel C, Chen H, Harold Li H, Low D, Moore K, et al. Clinical evaluation of a commercial orthopedic metal artifact reduction tool for CT simulations in radiation therapy. *Med Phys* 2012; **39**: 7507–17. doi: 10.1118/1.4762814

13. Andersson KM, Ahnesjö A, Vallhagen Dahlgren C. Evaluation of a metal artifact reduction algorithm in CT studies used for proton radiotherapy treatment planning. *J Appl Clin Med Phys* 2014; **15**: 4857. doi: 10.1120/jacmp.v15i5.4857

14. Prell D, Kalender WA, Kyriakou Y. Development, implementation and evaluation of a dedicated metal artefact reduction method for interventional flat-detector CT. *Br J Radiol* 2010; **83**: 1052–62. doi: 10.1259/bjr/19113084

15. *Metal artefact reduction for orthopedic implants (O-MAR)*. Cleveland, OH: Philips Healthcare; 2012 [cited 8 January 2012]. Available from: http://clinical.netforum.healthcare.philips.com/us_en/Explore/White-Papers/CT/Metal-Artefact-Reduction-for-Orthopedic-Implants-(O-MAR)

16. Han SC, Chung YE, Lee YH, Park KK, Kim MJ, Kim KW. Metal artifact reduction software used with abdominopelvic dual-energy CT of patients with metal hip prostheses: assessment of image quality and clinical feasibility. *AJR Am J Roentgenol* 2014; **203**: 788–95. doi: 10.2214/AJR.13.10980